



Contents lists available at SciVerse ScienceDirect

Catalysis Today

journal homepage: [www.elsevier.com/locate/cattod](http://www.elsevier.com/locate/cattod)

## Ethanol steam reforming at very low temperature over cobalt talc in a membrane reactor

M. Domínguez<sup>a,b</sup>, E. Taboada<sup>a</sup>, E. Molins<sup>c</sup>, J. Llorca<sup>a,b,\*</sup><sup>a</sup> Institut de Tècniques Energètiques, Universitat Politècnica de Catalunya, Diagonal 647, Ed. ETSEIB, 08028 Barcelona, Spain<sup>b</sup> Centre for Research in Nanoengineering, Universitat Politècnica de Catalunya, Pasqual i Vila 15, 08028 Barcelona, Spain<sup>c</sup> Institut de Ciència de Materials de Barcelona, Consejo Superior de Investigaciones Científicas, Campus de la UAB, 08193 Bellaterra, Spain

### ARTICLE INFO

#### Article history:

Received 30 August 2011  
Received in revised form 24 January 2012  
Accepted 1 February 2012  
Available online xxx

#### Keywords:

Hydrogen  
Reforming  
Ethanol  
Pd dense membrane  
Catalytic membrane reactor

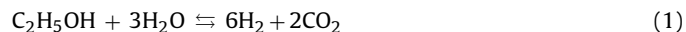
### ABSTRACT

Ethanol steam reforming has been carried out at low temperature in a catalytic membrane reactor consisting of cobalt talc ( $\text{Co}_3[\text{Si}_2\text{O}_5]_2(\text{OH})_2$ ) supported over cordierite and a Pd–Ag membrane. No sweep gas has been used, therefore, pure hydrogen has been obtained in the permeate stream, which has been maintained at atmospheric pressure. The configuration with the catalyst bed packed around the membrane has shown superior performance than the staged configuration, where the honeycomb catalyst has been placed in-series with the membrane. The influence of the temperature (598–673 K) and the pressure inside the reactor (5–15 bar) on different parameters such as the hydrogen production and the pure hydrogen recovery has been evaluated. The catalytic membrane reactor device has a rapid response to changes in the ethanol–water liquid mixture load; a constant hydrogen flow has been obtained after 2 s following variations of  $\pm 10\%$ .

© 2012 Elsevier B.V. All rights reserved.

### 1. Introduction

The development of proton exchange membrane fuel cells (PEMFCs) for the market of power sources for portable and mobile applications has moved researchers to investigate in the development of small scale fuel reformers for on-site hydrogen generation from various liquid fuels as an alternative to direct hydrogen storage [1,2]. Among liquid fuels that are currently considered, ethanol is particularly appealing since it is a renewable source when obtained from biomass, it is easy to handle and distribute and it is readily available [3]. In recent years, numerous catalyst formulations have been studied intensively for ethanol steam reforming (ESR) aiming at the generation of hydrogen [4–6]:



A survey of the literature reveals that noble metal-based catalysts perform well for ESR [7–9]. They are stable and exhibit high activity, but only at high temperature. The reason is that the reaction mechanism involves the decomposition of ethanol at moderate temperature into a mixture of hydrogen, carbon monoxide and methane (Eq. (2)), followed by the water gas shift reaction (WGS,

Eq. (3)) and, finally, the steam reforming of methane at high temperature (Eq. (4)):



In contrast, cobalt-based catalysts can operate at a much lower temperature, typically at 673–823 K, since they do not yield methane as an intermediate species in the reaction mechanism, which can only be reformed at high temperature [10–38]. Over cobalt-based catalysts, ethanol is first dehydrogenated at low temperature into a mixture of hydrogen and acetaldehyde (Eq. (5)), and acetaldehyde reacts with steam to yield mainly hydrogen and carbon oxides (Eq. (6)), which participate in the WGS (Eq. (3)), or decompose into carbon monoxide and methane (Eq. (7)):



Recently, we have reported that cobalt talc ( $\text{Co}_3[\text{Si}_2\text{O}_5]_2(\text{OH})_2$ ) is active and selective to carry out the ESR even at a lower temperature [39,40]. At 623 K, a reformat composition of 68.7%  $\text{H}_2$ , 23.2%  $\text{CO}_2$ , 1.0%  $\text{CO}$  and 7.1%  $\text{CH}_4$  is measured at steam-to-carbon ratio of  $S/C = 1.5$  (stoichiometric ethanol–water mixture, Eq. (1)) and full

\* Corresponding author at: Institut de Tècniques Energètiques, Universitat Politècnica de Catalunya, Av. Diagonal 647, Ed. ETSEIB, 08028 Barcelona, Spain. Tel.: +34 93 401 17 08; fax: +34 93 401 71 49.

E-mail address: [jordi.llerca@upc.edu](mailto:jordi.llerca@upc.edu) (J. Llorca).

ethanol conversion [39]. In addition, the catalyst exhibits fast start-up (few seconds) and a stable reformat composition is obtained, even after shut-down and exposure to air up to 613 K. High resolution transmission electron microscopy, X-ray diffraction, magnetic measurements and in situ X-ray photoelectron spectroscopy experiments [41] have revealed that cobalt talc undergoes delamination into individual nanolayers under reaction conditions and, simultaneously, metal cobalt ensembles segregate at the surface of the nanolayers facilitating the redox pair  $\text{Co}^0 \rightleftharpoons \text{Co}^{2+}$ , thus offering a composite material with high surface area and reactivity, which accounts for the outstanding catalytic behavior observed. In addition, cobalt talc is a material with low acidity/basicity and prevents dehydration of ethanol into ethylene, which is a coke precursor that causes deactivation.

An important advantage of conducting the ESR at low temperature is that the WGS equilibrium favors the formation of hydrogen and  $\text{CO}_2$  at the expense of CO and water (Eq. (3)), thus maximizing the production of  $\text{H}_2$  and avoiding the requirement of additional WGS units at the reactor outlet. This condition considerably simplifies the fuel processor design, both in terms of number of catalytic stages required as well as heat transfer management. The reformat can enter directly into a CO clean-up unit (CO preferential oxidation and/or methanation) prior to feed the PEMFC anode. However, the reformat gas mixtures contain, in addition to hydrogen and CO, large amounts of  $\text{CO}_2$  and  $\text{CH}_4$  and minor amounts of other hydrocarbons ( $\text{C}_2\text{H}_4$ ,  $\text{C}_2\text{H}_6$ , ...) and oxygenates ( $\text{CH}_3\text{COCH}_3$ , ...), which require additional separation steps. In this context, the use of catalytic membrane reactors (CMRs), where the generation and separation of hydrogen take place simultaneously, appears as an attractive approach to simplify on-site reformers. In addition, the shift effect that occurs in CMR results in even higher hydrogen yields. Among them, Pd-based membrane reactors fulfill the requirements to obtain an ultra pure hydrogen stream suitable for PEMFC feeding [42–45]. There is information available in the literature on the steam reforming of ethanol in CMR with palladium–alloy membranes [46–51], but these are mostly limited to high temperature operation. Given its potential use for on-site, on-demand hydrogen generation at low temperature in ethanol processors for fuel cell feeding in portable and mobile applications, here we describe the performance of cobalt talc in a dense Pd–Ag membrane reactor for producing pure hydrogen.

## 2. Experimental

### 2.1. Preparation of catalyst

Cordierite monoliths (Corning, 400 cpsi) were used as a catalyst support.  $\text{Co}_3[\text{Si}_2\text{O}_5(\text{OH})_2]$  was grown over the cordierite pieces by a sol–gel method followed by supercritical drying [39]. First, the cordierite pieces were coated with a thin layer of silica alcogel through the hydrolysis and condensation of tetraethoxysilane (TEOS,  $\text{Si}(\text{OCH}_2\text{CH}_3)_4$ , 98% Sigma Aldrich) dissolved in ethanol. Gelation was catalyzed by addition of an aqueous solution of  $\text{HNO}_3$ –HF (molar ratio  $\text{TEOS}:\text{EtOH}:\text{H}_2\text{O}:\text{HNO}_3:\text{HF} = 1.0:6.0:15.9:0.03:0.12$ ). Next, the alcogel was impregnated with a saturated ethanolic solution of cobalt nitrate hexahydrate ( $\text{Co}(\text{NO}_3)_2 \cdot 6\text{H}_2\text{O}$ , 99% Scharlau) during 24 h. Finally, the solvent was extracted under supercritical conditions at  $6.28 \times 10^6$  Pa and 516 K, which resulted in the formation of a thin layer of cobalt talc over the cordierite surface [39]. The catalyst was activated by performing two consecutive cycles of 473–773–623 K under a  $\text{C}_2\text{H}_5\text{OH}:\text{H}_2\text{O}$  atmosphere in order to delaminate the cobalt talc structure and segregate metal cobalt ensembles on the surface as explained previously [40]. The microstructure, morphology, and composition of the catalyst layer

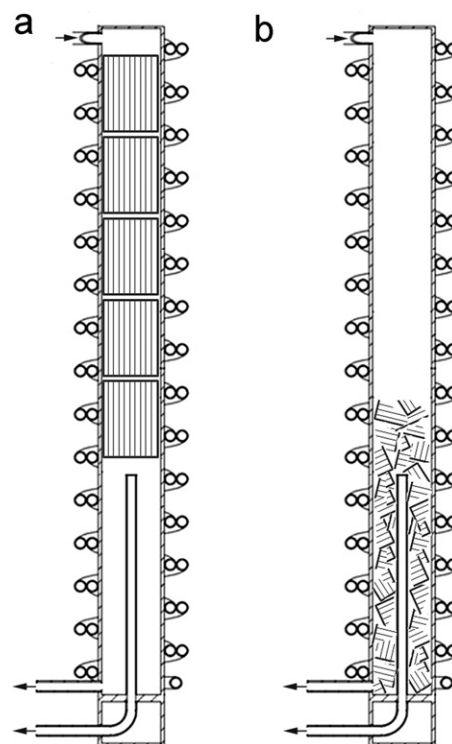
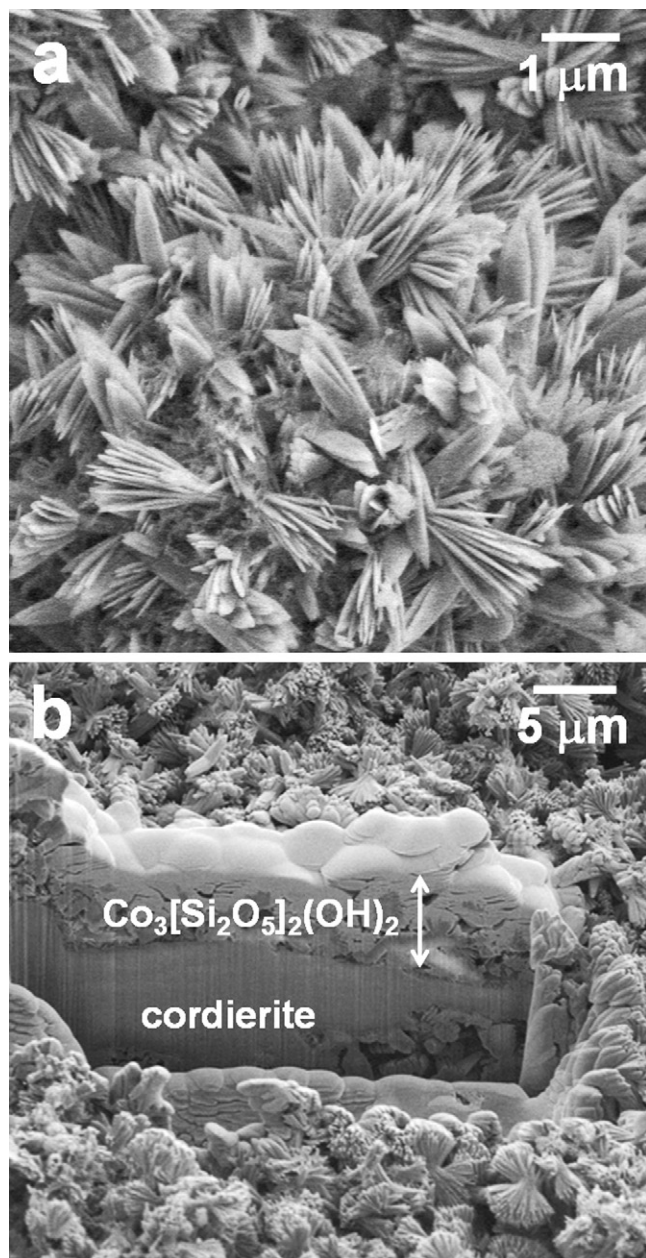


Fig. 1. Scheme of the two membrane reactor configurations tested. (a) Staged membrane reactor and (b) catalytic membrane reactor.

were studied with a Zeiss NEON40 crossbeam scanning electron microscope (SEM) operated at 5 kV and equipped with energy dispersive X-ray (EDX) analysis and focus ion beam (FIB).

### 2.2. Reaction tests

The functionalized cordierite pieces described above were implemented in a membrane reactor machined in stainless steel measuring 230 mm tall and 22 mm OD (Reb Research & Consulting). A feed evaporation conduit was welded around the reactor. The membrane was a 76 mm tall, 1/8 in. diameter, pine-hole free, dead-end tube with a total area of  $7.1 \text{ cm}^2$ . The thickness of the Pd–Ag active layer measured  $30 \mu\text{m}$ . Two configurations of the catalytic membrane reactor were selected. First, the catalytic monoliths were disposed in-series into the reactor followed by the membrane tube (Fig. 1a), resulting in a staged membrane reactor. In the second configuration, the same catalytic monoliths were crushed into small pieces (ca. 5 mm) and distributed around the membrane tube (Fig. 1b). The liquid feed mixture of ethanol and water was pumped into the reactor module and adjusted to attain a S/C ratio of 3 ( $\text{C}_2\text{H}_5\text{OH}:\text{H}_2\text{O} = 1:6$  molar). The retentate pressure was adjusted by a manually operated back-pressure regulator. No pressure regulation was implemented on the permeate side (atmospheric pressure). No sweep gas was used, therefore, pure hydrogen was obtained in the permeate stream. The gaseous products of the retentate were analyzed by online gas chromatography (Agilent 3000A MicroGC) using MS 5 Å, PlotU and Stabilwax columns, as well as the permeate to verify the selectivity of the membrane separation towards hydrogen. Total volumetric flowrates of both permeate (Bronkhorst EL-FLOW) and dry retentate streams (bubble meter) were measured. By measuring under steady-state conditions and in a precise period of time both the composition and flowrate of the gaseous outlet streams as well as the volume of liquid condensed from the retentate flow we verified the correct closure of the mass balance. Before the reaction, pure gas



**Fig. 2.** Scanning electron microscopy (SEM) images of the cobalt talc catalyst particles supported over the cordierite substrate (a) and after cutting with the focus ion beam (FIB) technique to determine the thickness of the catalytic layer (b).

permeation tests were carried out on the reactor membrane in the temperature range of 573–673 K, which showed that the selectivity towards hydrogen was infinite and that both Sievert's and Arrhenius' laws were followed. The apparent activation energy was found to be equal to  $2.9 \text{ kJ mol}^{-1}$ , which are fairly similar to experimental data found in literature for the same kind of membranes [49].

### 3. Results and discussion

#### 3.1. Catalyst characterization and activation

Fig. 2a shows a representative SEM image of the  $\text{Co}_3[\text{Si}_2\text{O}_5]_2(\text{OH})_2$  catalytic layer over the cordierite support. The dispersion of catalyst was very homogeneous over the cordierite pieces. As expected from the crystalline structure of cobalt talc, platelet morphology was evident for the catalyst

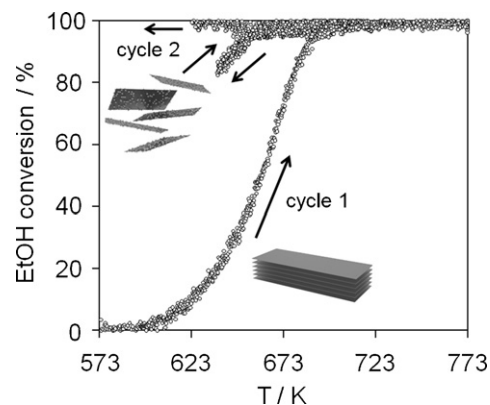


**Fig. 3.** Ethanol conversion during two consecutive activation cycles of the cobalt talc catalyst.

particles, which formed agglomerates of about 3–5  $\mu\text{m}$ . Individual platelets measured ca.  $2 \mu\text{m} \times 0.3 \mu\text{m} \times 0.03 \mu\text{m}$ . The thickness of the cobalt talc layer over the cordierite pieces was evaluated after cutting the catalyst layer with an Ar ion beam (Fig. 2b). The cut was oriented perpendicular to the catalytic layer and was performed after sputtering with Pt in order to get a sharp edge. The mean thickness of the catalytic layer measured was in the range 4–6  $\mu\text{m}$ .

Before performing the catalytic tests in the membrane reactor, the  $\text{Co}_3[\text{Si}_2\text{O}_5]_2(\text{OH})_2$  catalyst supported over the cordierite honeycomb pieces was activated in an open tubular reactor. The activation treatment was carried out at atmospheric pressure with an ethanol–water atmosphere in an inert stream. Two consecutive cycles were performed between 473 and 773 K at  $10 \text{ K min}^{-1}$ . Fig. 3 shows the ethanol conversion measured during the activation treatment. During the first part of cycle 1, the ethanol started to transform at 573 K and it was completely reformed at 723 K. In the second part of cycle 1, during cooling down, the catalyst was partially activated and the conversion of ethanol was total above 648 K. The activation was completed after cycle 2, when ethanol was fully reformed at temperatures as low as 598 K. As discussed in [41], cobalt talc undergoes activation through delamination and formation of metal cobalt ensembles at the surface of the nanolayers.

#### 3.2. Effect of reactor configuration

As explained in the experimental section, two configurations for the catalyst and the Pd–Ag separation membrane were tested in the same reactor under the same reaction conditions (Fig. 1). Table 1 compiles the ethanol conversion values attained in both cases as well as the hydrogen yield at 8 bar and 598–673 K. Under the ethanol load tested,  $600 \text{ g}_{\text{cat}} \text{ min mol}_{\text{EtOH}}^{-1}$ , the ethanol

**Table 1**

Conversion of ethanol and hydrogen yield obtained at different temperature and 8 bar in the staged membrane reactor and catalytic membrane reactor configurations.  $W/F = 600 \text{ g}_{\text{cat}} \text{ min mol}_{\text{EtOH}}^{-1}$ .

Configuration	T (K)	conv <sub>EtOH</sub> (%)	mol <sub>H<sub>2</sub></sub> /mol <sub>EtOH,in</sub>
Staged MR	598	73.6	0.6
	623	91.5	1.3
	648	95.8	2.1
	673	97.8	2.8
Catalytic MR	598	98.6	3.2
	623	100	3.5
	648	100	3.6
	673	100	3.7

conversion was incomplete in the staged membrane reactor configuration (Fig. 1a), whereas ethanol was fully converted at 623 K in the catalytic membrane reactor configuration (Fig. 1b). As expected, in both cases the ethanol conversion increased with temperature due to the endothermic nature of the process. In the catalytic membrane reactor configuration the yield of hydrogen reached 3.5–3.7 mol<sub>H<sub>2</sub></sub>/mol<sub>EtOH,in</sub> at 623–673 K, much higher than the corresponding values obtained in the staged membrane reactor configuration (1.3–2.8 mol<sub>H<sub>2</sub></sub>/mol<sub>EtOH,in</sub>). Although the ethanol conversion level became similar at high temperature (648–673 K) for both configurations, the difference in hydrogen yield was due mainly to the presence of acetaldehyde (the first step in ethanol reforming over Co-based catalysts, Eq. (5)) and dimethylketone (which is formed through condensation of acetaldehyde on the basic sites of cobalt talc) in the staged membrane reactor configuration. Therefore, it is concluded that the performance of the membrane reactor configuration, where reaction and selective separation of hydrogen occurs simultaneously, is much better than that of the staged membrane reactor configuration, where reaction and hydrogen separation are separate, consecutive steps. The continuous removal of hydrogen in the catalytic membrane reactor configuration permits obtaining not only ethanol conversion values higher than those recorded over the staged membrane reactor configuration (shift effect), but also the completion of the reforming process, overall resulting in higher hydrogen yields, even if back permeation of hydrogen can occur in this configuration [52]. Taking into account these results, only the catalytic membrane reactor configuration was considered for further studies.

### 3.3. Effect of temperature

The effect of temperature on the distribution of products was studied at a gauge pressure of 7.5 bar and at a constant ethanol load of 600 g<sub>cat</sub> min mol<sub>EtOH</sub><sup>-1</sup> and S/C=3. Fig. 4a shows the selectivity on a dry basis of the products obtained in the temperature range 598–673 K. The error bars indicate data dispersion during independent experiments. Only hydrogen, carbon oxides (CO and CO<sub>2</sub>) and methane were obtained. No ethylene and other hydrocarbons were detected. The amount of hydrogen increased progressively with temperature at the expense of methane, which is explained in terms of methane steam reforming (Eq. (4)). On the other hand, as temperature was increased, the reverse water gas shift reaction was favored and the amount of CO increased at the expense of CO<sub>2</sub>, according to the WGS equilibrium (Eq. (3)). The amount of hydrogen permeated was about 30–32 STP mL min<sup>-1</sup> and it was maintained virtually constant in the range of temperature used, indicating that temperature had a small effect on hydrogen recovery under the conditions tested.

### 3.4. Effect of pressure

Pressure had also a small effect on the distribution of products of the reaction, but it affected strongly the production and separation of hydrogen. Fig. 4b shows the distribution of products on a dry basis obtained at a fixed temperature of 623 K. The variation of the reactor pressure barely affected the WGS equilibrium and the amounts of CO and CO<sub>2</sub> remained approximately constant. The selectivity towards methane progressively increased with pressure at the expense of hydrogen, which is explained in terms of the Le Chatelier's principle, since the consumption of moles of H<sub>2</sub> and CO<sub>x</sub> is favored with pressure to yield CH<sub>4</sub>. It is interesting to remark that since reforming at higher pressures favor methane formation, the removal of hydrogen from the reforming zone in the catalytic membrane reactor configuration shifted the reaction towards lower formation of methane leading to higher hydrogen yields with respect to the staged membrane reactor configuration.

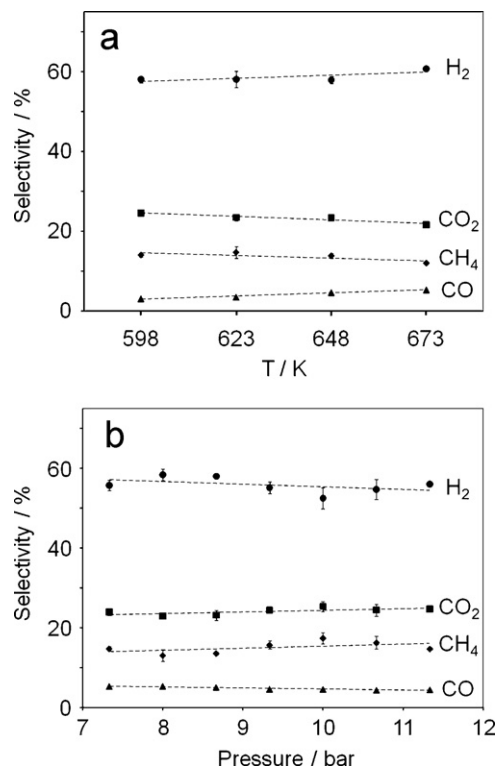
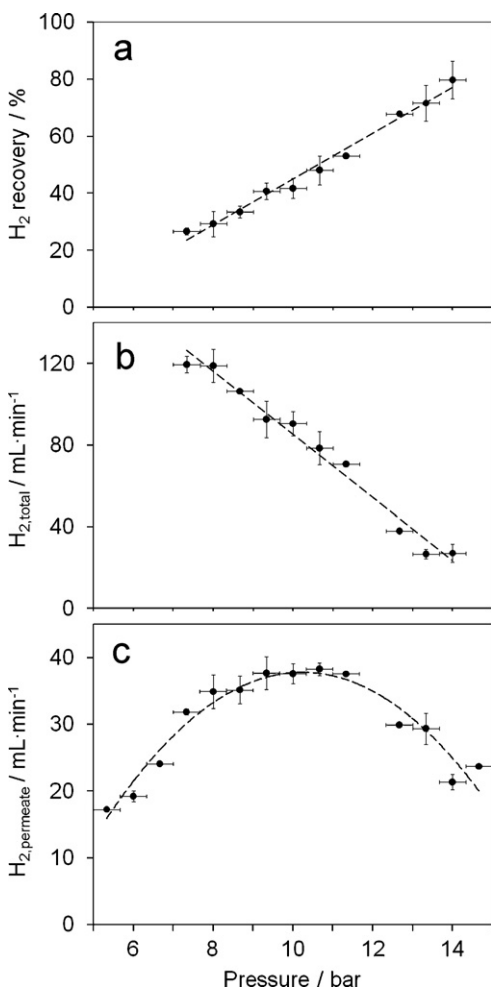


Fig. 4. Product distribution obtained at different temperature (a, fixed gauge pressure of 7.5 bar) and gauge pressure (b, fixed temperature of 623 K) in the catalytic membrane reactor configuration. W/F=600 g<sub>cat</sub> min mol<sub>EtOH</sub><sup>-1</sup>, S/C=3.

At a gauge pressure of 7.5 bar, a methane selectivity value of 22.5% was recorded in the staged membrane reactor whereas for the catalytic membrane reactor methane selectivity was considerably lower, about 15%.

Hydrogen recovery, defined as 100(F<sub>H<sub>2</sub>,permeate</sub>/F<sub>H<sub>2</sub>,produced</sub>), was strongly dependent on the reactor pressure. Fig. 5a shows the amount of hydrogen recovered at different pressure values. There is a linear trend between hydrogen recovery and pressure in the range tested, and recovery values as high as 80% were attained at a gauge pressure of 14 bar. The increase of hydrogen recovery through the membrane is explained in terms of the hydrogen permeation driving force due to the difference in hydrogen pressure at both sides of the membrane, as expected from the Richardson equation. The larger the pressure difference of hydrogen in the retentate and permeate sides, the larger the hydrogen recovered in the permeate side. However, the pressure increase produced two conflicting effects. As explained above, a higher hydrogen permeating flux was obtained at higher pressure values but, at the same time, a decrease in the total production of hydrogen (F<sub>H<sub>2</sub>,retentate</sub>/F<sub>H<sub>2</sub>,permeate</sub>) was observed (Fig. 5 b). This is a direct consequence of the thermodynamics of the reaction since the complete ethanol steam reforming reaction proceeds with a strong increase of the moles number (Eq. (1)). This negative effect on the yield of hydrogen showed also a linear trend. Therefore, a plot of the amount of hydrogen recovered (F<sub>H<sub>2</sub>,permeate</sub>) against reactor pressure exhibits a volcano-type shape, as shown in Fig. 5c. At gauge pressure values below 8–9 bar, the amount of hydrogen recovered increased with pressure, which means that the membrane effect overcome the thermodynamic one, while the opposite is true for gauge pressure values higher than ca. 11 bar. Under the conditions tested, the maximum hydrogen recovery was attained at a gauge pressure of about 10 bar, where 1.4 STP L<sub>H<sub>2</sub>,permeate</sub> mL<sub>EtOH,liquid</sub><sup>-1</sup> were generated.



**Fig. 5.** Hydrogen recovered (a), hydrogen produced (b) and hydrogen permeated (c) at 623 K and different gauge pressure.  $W/F = 600 \text{ g}_{\text{cat}} \text{ min mol}_{\text{EtOH}}^{-1}$ ,  $S/C = 3$ .

### 3.5. Dynamic response

It has been reported that cobalt talc catalyst exhibits fast response to changes in the operation parameters [39]. This has been one of the reasons to use this catalyst in this work, as explained in the introduction. To check for application purposes in portable and/or mobile environments, where fast dynamic response is crucial, a study of the dynamic response of the catalytic membrane reactor upon changes in the ethanol + water load was carried out. In a typical experiment, the pure hydrogen flow (permeate) was measured continuously with a mass flow meter; at steady state, the ethanol load was changed by varying the liquid pump flow and the hydrogen flow monitored until steady state was reached again. Two variables were measured: the time elapsed between the new set point of the liquid pump and the dispersion around the mean hydrogen flow. Fig. 6 shows the hydrogen flow recorded against time following an increase of 10% in the ethanol load (from  $1.50 \times 10^{-3} \text{ mol}_{\text{EtOH}} \text{ min}^{-1}$  to  $1.65 \times 10^{-3} \text{ mol}_{\text{EtOH}} \text{ min}^{-1}$ ) at a gauge pressure of 7.5 bar and 623 K. The time elapsed between the two steady states was only 2–3 s. On the other hand, the dispersion around the mean hydrogen flow at each steady state level was always around 2%, independently of the hydrogen flow. Overall, the membrane reactor loaded with the cobalt talc catalyst has shown a high dynamic response upon changes in the ethanol load, thus providing a robust system for the on-site, on-demand generation of hydrogen. However, it should be mentioned that carbon deposition was observed at the end of the experiments ( $0.03 \text{ g}_{\text{C}} \text{ g}_{\text{catalyst}}^{-1} \text{ h}^{-1}$ ).

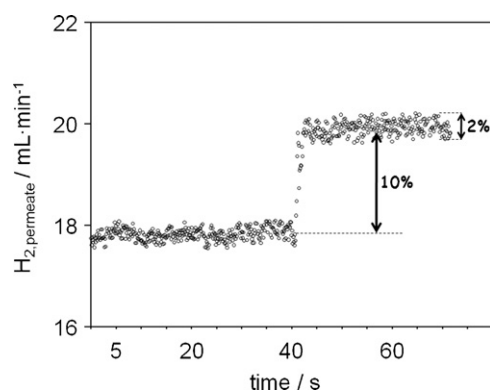


**Fig. 6.** Hydrogen permeated in the cobalt talc catalytic membrane reactor following a 10% increase in the ethanol load (from  $1.50 \times 10^{-3}$  to  $1.65 \times 10^{-3} \text{ g}_{\text{cat}} \text{ min mol}_{\text{EtOH}}^{-1}$ ,  $S/C = 3$ ).

### 3.6. Energy balance considerations

Steam reforming reactions are endothermic. In the case of the ethanol steam reforming, it is also necessary to vaporize all the reactants (water and ethanol) and heat them up to the reaction temperature, resulting even in a more heat-demanding process. In our membrane reactor, we have seen that the optimum operating gauge pressure is about 10 bar, which results in hydrogen recovery values of about 50%, which means that an important part of the hydrogen produced is not recovered in the permeate side. One way to supply the heat required for the process is to burn the off-gas of the membrane reactor (retentate side) which, in addition to hydrogen not recovered, it also contains methane and carbon monoxide that can be also combusted (a typical off-gas composition is ca. 39%  $\text{H}_2$ , 33%  $\text{CO}_2$ , 22%  $\text{CH}_4$  and 6%  $\text{CO}$ ). At 673 K and at a gauge pressure of 10 bar,  $0.48 \text{ L}_{\text{H}_2, \text{pure}} \text{ min}^{-1}$  are produced from an ethanol load of  $1 \text{ g}_{\text{EtOH}} \text{ min}^{-1}$ , which corresponds to ca. 32 W PEM fuel cell. The amount of heat required for ethanol and water vaporization and heating is 170 W, and the heat required for the reaction under these conditions is 34 W. Therefore, the heat required is 204 W, which is much higher than the 32 W that the PEM fuel cell yields. However, the combustion of the off-gas can account for 201 W, which is nearly the heat requirement of the process. Obviously, heat losses would occur in any practical device and the heat released by the combustion of the off-gas would not be sufficient for the process. This can be overcome by using lower excess of water; by decreasing the  $S/C$  from 3 to 2, the heat requirement of the process would decrease ca. 25%.

### 4. Conclusions

Cobalt talc ( $\text{Co}_3[\text{Si}_2\text{O}_5]_2(\text{OH})_2$ ) was supported over cordierite pieces and placed inside a membrane reactor with a single, dead-end Pd–Ag membrane in two configurations. In one configuration, the catalyst pieces were placed in-series with the membrane, forming a staged membrane device. In the second configuration, the catalyst was packed around the membrane, forming a catalytic membrane reactor. Ethanol steam reforming with  $S/C = 3$  was carried out in both configurations at different temperature and pressure. The catalytic membrane reactor configuration showed both higher ethanol conversion and higher selectivity towards hydrogen due to the shift effect. No sweep gas was used, therefore, pure hydrogen was obtained in the permeate stream, which was maintained at atmospheric pressure. At full ethanol conversion, temperature had a little effect on selectivity and hydrogen separation. In contrast, the retentate pressure had a strong influence on hydrogen yield and recovery. The increase in pressure produced

two conflicting effects. On one hand, a higher hydrogen permeating flux was obtained but, on the other hand, a decrease in the total production of hydrogen was observed due to the thermodynamics of the reaction. Therefore, a plot of the amount of hydrogen recovered against reactor pressure showed a volcano-type shape, with a maximum hydrogen recovery occurring at a gauge pressure of about 10 bar. The cobalt talc membrane reactor exhibited a rapid response to changes in the ethanol-water liquid mixture load, thus suggesting that this type of device is of interest for the development of ethanol fuel processors for portable applications.

### Acknowledgments

This work has been funded through MICINN grant CTQ2009-12520. M.D. acknowledges an FI grant from Generalitat de Catalunya and European Social Fund. E.T. acknowledges a postdoctoral grant from UPC. J.L. is grateful to ICREA Academia program.

### References

- [1] G. Kolb, *Fuel Processing for Fuel Cells*, Wiley-VCH, Weinheim, 2008, pp.1–434.
- [2] J. Llorca, *Microreactors for the generation of hydrogen from ethanol*, in: W.H. Lee, V.G. Cho (Eds.), *Handbook of Sustainable Energy*, Nova Publishers, 2010, pp. 693–699 (Chapter 22).
- [3] M. Murdoch, G.I.N. Waterhouse, M.A. Nadeem, J.B. Metson, M.A. Keane, R.F. Howe, J. Llorca, H. Idriss, *Nat. Chem.* 3 (2011) 489.
- [4] P.D. Vaidya, A.E. Rodrigues, *Chem. Eng. J.* 117 (2006) 39.
- [5] A. Haryanto, S. Fernando, N. Murali, S. Adhikari, *Energy Fuels* 19 (2005) 2098.
- [6] M. Ni, Y.C. Leung, M.K.H. Leung, *Int. J. Hydrogen Energy* 32 (2007) 3238.
- [7] G.A. Deluga, J.R. Salge, L.D. Schmidt, X.E. Verykios, *Science* 303 (2004) 993.
- [8] F. Frusteri, S. Freni, *J. Power Sources* 173 (2007) 200.
- [9] H. Idriss, M. Scott, J. Llorca, S.C. Chan, W. Chiu, P.Y. Sheng, A. Yee, M.A. Blackford, S.J. Pas, A.J. Hill, F.M. Alamgir, R. Rettew, C. Petersburg, S. Senanayake, M.A. Barteau, *ChemSusChem* 1 (2008) 905.
- [10] F. Haga, T. Nakajima, H. Miya, S. Mishima, *Catal. Lett.* 48 (1997) 223.
- [11] J. Llorca, N. Homs, J. Sales, P. Ramírez de la Piscina, *J. Catal.* 209 (2002) 306.
- [12] J. Llorca, P. Ramírez de la Piscina, J.A. Dalmon, J. Sales, N. Homs, *Appl. Catal. B* 43 (2003) 355.
- [13] J. Llorca, J.A. Dalmon, P. Ramírez de la Piscina, M. Homs, *Appl. Catal. A* 243 (2003) 261.
- [14] S. Freni, S. Cavallaro, N. Mondello, L. Spadaro, F. Frusteri, *Catal. Commun.* 4 (2003) 259.
- [15] F. Mariño, G. Baronetti, M. Jobbagy, M. Laborde, *Appl. Catal. A* 238 (2003) 41.
- [16] J. Llorca, N. Homs, J. Sales, J.L.G. Fierro, P. Ramírez de la Piscina, *J. Catal.* 222 (2004) 470.
- [17] J. Llorca, P. Ramírez de la Piscina, J.A. Dalmon, N. Homs, *Chem. Mater.* 16 (2004) 3573.
- [18] J. Llorca, N. Homs, P. Ramírez de la Piscina, *J. Catal.* 227 (2004) 556.
- [19] M.S. Batista, R.K.S. Santos, E.M. Assaf, J.M. Assaf, E.A. Ticianelli, *J. Power Sources* 134 (2004) 27.
- [20] A. Kaddouri, C. Mazzocchia, *Catal. Commun.* 5 (2004) 339.
- [21] H. Song, L. Zhang, R.B. Watson, D. Braden, U. Ozkan, *Catal. Today* 129 (2007) 346.
- [22] J.A. Torres, J. Llorca, A. Casanovas, M. Domínguez, J. Salvadó, D. Montané, *J. Power Sources* 169 (2007) 158.
- [23] M. Benito, R. Padilla, L. Rodríguez, J.L. Sanz, L. Daza, *J. Power Sources* 169 (2007) 167.
- [24] S. Tutti, F. Pepe, *Catal. Lett.* 122 (2008) 196.
- [25] H. Song, U. Ozkan, *J. Catal.* 261 (2009) 66.
- [26] A. Casanovas, C. de Leitenburg, A. Trovarelli, J. Llorca, *Catal. Today* 138 (2008) 187.
- [27] A. Casanovas, M. Saint-Gerons, F. Griffon, J. Llorca, *Int. J. Hydrogen Energy* 33 (2008) 1827.
- [28] J. Llorca, A. Casanovas, T. Trifonov, A. Rodríguez, R. Alcubilla, *J. Catal.* 255 (2008) 228.
- [29] H. Wang, J.L. Ye, Y. Liu, Y.D. Li, Y.N. Qin, *Catal. Today* 129 (2007) 305.
- [30] J. Sun, X.-P. Qiu, F. Wu, W.-T. Zhu, *Int. J. Hydrogen Energy* 30 (2005) 437.
- [31] A.E. Galetti, M.F. Gomez, L.A. Arrua, A.J. Marchi, M.C. Abello, *Catal. Commun.* 9 (2008) 1201.
- [32] J.C. Vargas, S. Libs, A.C. Roger, A. Kiennemann, *Catal. Today* 107 (2005) 417.
- [33] A. Casanovas, M. Domínguez, C. Ledesma, E. López, J. Llorca, *Catal. Today* 143 (2009) 32.
- [34] R. Nedyalkova, A. Casanovas, J. Llorca, D. Montané, *Int. J. Hydrogen Energy* 34 (2009) 2591.
- [35] A. Casanovas, C. de Leitenburg, A. Trovarelli, J. Llorca, *Chem. Eng. J.* 154 (2009) 267.
- [36] E. López, A. Irigoyen, T. Trifonov, A. Rodríguez, J. Llorca, *Int. J. Hydrogen Energy* 35 (2010) 3472.
- [37] A. Casanovas, M. Roig, C. de Leitenburg, A. Trovarelli, J. Llorca, *Int. J. Hydrogen Energy* 35 (2010) 7690.
- [38] P. Bichon, G. Haugom, H.J. Venvik, A. Colmen, E.A. Blekkan, *Top. Catal.* 49 (2008) 38.
- [39] M. Domínguez, E. Taboada, E. Molins, J. Llorca, *Catal. Today* 138 (2008) 193.
- [40] M. Domínguez, G. Cristiano, E. López, J. Llorca, *Chem. Eng. J.* 176–177 (2011) 280–285.
- [41] M. Domínguez, E. Taboada, H. Idriss, E. Molins, J. Llorca, *J. Mater. Chem.* 20 (2010) 4875.
- [42] A. Basile, *Top. Catal.* 51 (2008) 107.
- [43] S. Tosti, A. Basile, L. Bettinali, F. Borgognoni, F. Gallucci, C. Rizzello, *Int. J. Hydrogen Energy* 33 (2008) 5098.
- [44] A. Basile, F. Gallucci, A. Iulianelli, S. Tosti, *Fuel Cells* 8 (2008) 62.
- [45] G.S. Burkhanov, N.B. Gorina, N.B. Kolchugina, N.R. Roshan, *Platinum Met. Rev.* 55 (2011) 3.
- [46] G. Manzolini, S. Tosti, *Int. J. Hydrogen Energy* 33 (2008) 5571.
- [47] D. Papadias, D. Lee, H.D. Sheldon, M. Ferrandon, S. Ahmed, *Int. J. Hydrogen Energy* 35 (2010) 2004.
- [48] F. Gallucci, M. De Falco, S. Tosti, L. Marrelli, A. Basile, *Int. J. Hydrogen Energy* 33 (2008) 6165.
- [49] S. Tosti, A. Basile, F. Borgognoni, V. Capaldo, S. Cordiner, S. Di Cave, F. Gallucci, C. Rizzello, A. Santucci, E. Traversa, *J. Membr. Sci.* 308 (2008) 250.
- [50] C.Y. Yu, D.W. Lee, S.J. Park, K.Y. Lee, K.H. Lee, *Int. J. Hydrogen Energy* 34 (2009) 2947.
- [51] S. Tosti, A. Basile, R. Borelli, F. Borgognoni, S. Castelli, M. Fabbri, F. Gallucci, C. Licusati, *Int. J. Hydrogen Energy* 34 (2009) 4747.
- [52] G. Barbieri, A. Brunetti, G. Tricoli, E. Drioli, *J. Power Sources* 182 (2008) 160.